Journal of Functional Foods 121 (2024) 106420

Contents lists available at ScienceDirect

Journal of Functional Foods

journal homepage: www.elsevier.com/locate/jff

In vitro anti-inflammatory activity of *Malus* × *domestica* var. Mela Rosa Marchigiana pulp callus extract contrasting high glucose conditions

Leila Benayada [a,1], Federica Gubitosa [a,1], Daniele Fraternale [a], Silvia Carloni [a], Liana Cerioni [a], Giulia Matacchione [b], Fabiola Olivieri [b,c], Lucia Potenza [a], Roberta De Bellis [a], Laura Chiarantini [a], Carla Roselli [a], Laura Valentini [a], Pietro Gobbi [a], Walter Balduini [a], Noemi Pappagallo [a], Natascia Ventura [d], George E.N. Kass [e], Mariastella Colomba [a,*,1], Maria Cristina Albertini [a,*,1]

[a] *Department of Biomolecular Sciences, University of Urbino Carlo Bo, 61029 Urbino, Italy*
[b] *Center of Clinical Pathology and Innovative Therapy, IRCCS INRCA, Ancona, Italy*
[c] *Department of Clinical and Molecular Sciences, Università Politecnica delle Marche, Ancona, Italy*
[d] *Medical Faculty, Institute of Clinical Chemistry and Laboratory Diagnostic, Heinrich Heine University and the IUF-Leibniz Research Institute for Environmental Medicine, 40225 Düsseldorf, Germany*
[e] *European Food Safety Authority (EFSA), 43126 Parma, Italy*

ARTICLE INFO

Keywords:
Apple
Ethanolic extract
Secondary metabolites
Pentacyclic triterpenic acids

ABSTRACT

The anti-inflammatory activity of the "Mela Rosa Marchigiana" (MRM) pulp callus ethanol Extract (MRME) was tested in different cellular models including (i) LPS-treated RAW 264.7; (ii) HUVEC exposed to short-term high Glucose (HG, 45 mM) or normal glucose (NG, 5 mM) concentrations; and (iii) HG (30 mN) and LPS-treated U937. To evaluate the anti-inflammatory effect of the extract, Nitric Oxide (NO) production was measured in RAW 264.6 cells, while IL-8, IL-1ß and MCP-1 expressions, along with modulation of some inflammation- or senescence-associated miRNAs (miR-21, miR-126, miR-17 and miR-217) were assessed in HUVECs and/or U937. MRME treatment reduced pro-inflammatory markers amount, suggesting a decreased generalised inflammatory response. Present findings indicate that MRME can contrast senescence- or HG-induced inflammation. Moreover, in HG- and LPS-induced inflammation, MRME reduced U937 monocyte activation by inhibiting mitochondrial respiration and inflammatory markers. Finally, the inhibitory potential of MRME on the digestive enzymes α-glucosidase, α-amylase and lipase activity was investigated. Our results support the idea that MRME has a positive effect on inhibition of endothelial/macrophage dysfunction under HG/senescence inflammatory conditions. Furthermore, the obtained results showed a modest inhibitory power of the extract (IC50 values: 2.98 ± 0.24, 1.77 ± 0.15, and 2.06 ± 0.31 mg/ml, respectively), which, however, could be of some help in decreasing the absorption of glucose and triglycerides.

1. Introduction

Plants, including food plants, are rich in various bioactive molecules which are considered to be a promising source for designing effective therapeutic agents. These molecules, also known as secondary metabolites (SMs), have been proven to promote human health by preventing the onset and progression of diseases (Martín Ortega & Segura Campos, 2019; Patil et al., 2009; Pillai et al., 2021; Shrinet et al., 2021). Unfortunately, one of the difficulties in obtaining SMs, including pentacyclic triterpenic acids (PTAs), is their limited availability in fresh

Abbreviations: AD, Alzheimer Disease; ETC, Electron Transport Chain, HG, High Glucose; HUVEC, Human Umbilical Endothelial Cells; LPS, Lipopolysaccharide; MRM, Mela Rosa Marchigiana; MRME, Mela Rosa Marchigiana callus Extract; NG, Normal Glucose; OXPHOS, Oxidative Phosphorylation System; PTAs, Pentacyclic Triterpenic Acids; ROS, Reactive Oxygen Species; SASP, Senescence-Associated Secretory Phenotype; SD, Standard Deviation; sHUVEC, senescent endothelial cells; SMs, Secondary Metabolites; T2D, Type 2 Diabetes; yHUVEC, young endothelial cells.

* Corresponding authors.
E-mail addresses: mariastella.colomba@uniurb.it (M. Colomba), maria.albertini@uniurb.it (M.C. Albertini).

[1] Equally contributed.

https://doi.org/10.1016/j.jff.2024.106420
Received 12 May 2024; Received in revised form 8 August 2024; Accepted 15 August 2024
Available online 24 August 2024

plant materials. Moreover, environmental factors or variables (such as light, temperature, soil water, soil fertility and salinity) can significantly affect some processes associated with plant growth and development, including the ability to synthesize SMs, thus eventually leading to different concentration and distribution of the bioactive molecules in different plants (Jäger et al., 2009). To overcome this issue, we developed a technique (patented in 2021; patent no. 102020000012466) to obtain cellular plant material *in vitro* (i.e., calluses) in a controlled environment, starting from explants of mature fruit pulp. Notably, calluses are characterized by the availability of material, affordability (i.e., the cultures are relatively cheap and easy to maintain), high yields of bioactive metabolites, and low environmental impact. Moreover, thanks to this technique, contrary to traditional methods, the production of phytochemicals is constant over time and, most of all, standardizable as being independent of seasonality and cultivation/preservation methods of plant drugs. Chemical analysis showed that, in the callus from fruit pulp, the content of some classes of SMs, such as PTAs, is significantly higher than in the starting plant material (Verardo et al., 2019). Since 2017, we started using this innovative method to obtain calluses from the ripe pulp of the local apple variety known as "Mela Rosa Marchigiana" (MRM) (*Malus* × *domestica* Borkh, Rosaceae family) which is distributed in the Marche region (Italy) at 400–900 m above sea level. Since then, the MRM pulp callus has been kept alive by a series of subcultures made every 28 days and its composition has periodically been characterized (Gubitosa et al., 2024; Potenza et al., 2020; Verardo et al., 2017). Extracts of MRM callus (MRME) have been demonstrated to contain a variety of PTAs (including oleanolic acid, ursolic acid, maslinic acid, corosolic acid, pomolic acid, annurcoic acid and tormentic acid) whose amounts are remarkably higher than those in fresh fruit pulp (Gubitosa et al., 2024; Wang et al., 2017b). Moreover, these SMs possess several biological activities including antiviral (Heidary Navid et al., 2014; Xiao et al., 2018), anti-inflammatory (Deng et al., 2021; Kashyap et al., 2016), antioxidant (Gubitosa et al., 2024; Potenza et al., 2020) and antidiabetic effects (Ding et al., 2018; Hibi et al., 2022; Lin et al., 2018; Miura et al., 2004; Xu et al., 2019). Nkuimi Wandjou et al. (Nkuimi Wandjou et al., 2020) showed that SMs, such as triterpenes and polyphenols derived from apple extracts, can modulate or inhibit the activity of physiological enzymes. Considering that (i) MRME composition includes several PTAs; (ii) PTAs have gained much attention due to their antihyperglycemic property, and (iii) type 2 diabetes (T2D, one of the most common age-related diseases) is characterised by abnormal glucose and lipid metabolism, it is tempting to speculate that MRME could help to counteract senescence and/or hyperglycaemic conditions. To test this hypothesis, we employed various experimental systems and approaches to assess the MRME effect on different aspects of cellular senescence and hyperglycaemic conditions. Considering the increasing effort in investigating natural compounds as active ingredients of functional food able to contribute to healthy ageing and prevent or delay age-associated chronic diseases, the present study was carried out to test whether MRME might have a positive effect on glucose-induced chronic inflammation and cellular senescence, which are two conditions both characterising T2D. To this aim, we preliminarily evaluated the anti-inflammatory activity of MRME in LPS-injured RAW 264.7 murine cells. Then, given that (i) HUVEC are commonly used *in vitro* as a model to study the effect of different pathological processes in the endothelium; (ii) replicative (i.e., senescent) HUVEC may be considered a model of endothelial dysfunction in many age-related diseases as they show a senescence-associated secretory phenotype (SASP) which characterizes senescent cells and can contribute to fuel inflammaging; and (iii) HUVEC were already employed in a study reporting on high glucose-induced inflammation in young (y) and senescent (s) endothelial cells (Matacchione et al., 2022), the same experimental system and the same experimental conditions were chosen to settle the most suitable (and simplest) *in vitro* model to simulate pathological blood glucose level and to test the potential of the extract. Thus, the effects of MRME on the regulation of inflammation in replicative HUVEC treated with a high concentration (HG, 45 mM) or normal concentration (NG, 5 mM) of glucose were evaluated. For each experimental group, changes in pro-inflammatory markers (IL-8, IL-1ß, MCP-1) expression levels and the modulation of a few selected miRNAs which emerged as critical regulators to control endothelial inflammation and senescence, were assessed. More specifically, endothelial inflammation is regulated by miRNAs such as miR-126 and miR-21 (Mone et al., 2023; Tang et al., 2023), while endothelial senescence is additionally controlled by other miRNAs, including miR-217 or miR-17 (Cao et al., 2024; Wang et al., 2021). Overexpression of miR-217 promotes endothelial senescence by acting as an endogenous inhibitor of SIRT1, while miR-217 inhibition delays senescence (Menghini et al., 2009; Qin et al., 2012; Zhang et al., 2024). MiR-17, is one of the six mature miRNAs encoded by the cluster miR-17–92 (Cao et al., 2024) and might have important roles in different types of diabetes since it is involved in various biological processes, including glucose homeostasis, insulin signaling, and pancreatic ß-cell function (Jiang et al., 2022).

Moreover, taking into account that the monocytes-macrophages are crucially important in T2D as they play a pivotal role in microvascular complications and inflammation observed in diabetic patients (Carantoni et al., 1997; Hoogerbrugge et al., 1996; Kim et al., 1994), U937 cells were used following (Haidet et al., 2012) as a monocytic cellular system to assess MRME effects in high glucose- and LPS-induced inflammation. In addition, inflammatory responses generating oxidative stress and endothelial dysfunction were investigated and the hypothesis that pre-exposure of U937 cells to MRME could prevent the inflammatory responses modulating the Oxidative Phosphorylation System (OXPHOS) was tested by High-Resolution Respirometry to monitor oxygen consumption in conditions of insult. Under these conditions, the same inflammatory markers detected in endothelial cells were measured.

Finally, considering that high levels of glucose and lipids are involved in diabetes development, we also investigated the inhibition potential of the extract on the digestive enzymes α-glucosidase and α-amylase (which play an important role in carbohydrates digestion) and lipase (which catalyses the hydrolysis of fats) to evaluate whether MRME could contribute to reduce the post-prandial increase of blood glucose and/or limit the digestion/absorption of dietary lipids.

2. Materials and methods

2.1. Mela Rosa Marchigiana callus extract (MRME) preparation

Ripe apples of the Mela Rosa Marchigiana (MRM) variety were collected from an orchard located in Urbino (Marche region, Italy) and processed to obtain the callus culture starting from ripe pulp explants (Wang et al., 2017b). Briefly, Gamborg B5 medium (Dixon, 1985) plus 2.0 mg/l BA (6-benzylaminopurine, Sigma-Aldrich) and 0.2 mg/l 2,4-D (2,4-dichlorophenoxyacetic acid, Sigma-Aldrich), 30 g/L sucrose, pH 5.8, induced the highest biomass production. Cultures were maintained in the dark at 25 ± 2 °C and subcultures were obtained after 28 days in the same media. Calli obtained by subcultures were stored at −20 °C and lyophilized before the extraction. The callus extract was obtained as described in Gubitosa et al. (Gubitosa et al., 2024), i.e., performing extra sequential resuspension (in 70 % ethanol) and centrifugation steps to minimize the debris as much as possible. Briefly, 260 mg of freeze-dried callus was extracted in 15 ml of 70 % EtOH for 15 min. The homogenate was stirred overnight at 4 °C and then centrifuged (45 min; 4 °C; 13,000*g*). After supernatant recovery, the pellet was extracted and centrifuged a second time, and the two supernatants were combined and dried in Savant overnight. The day after, 15 ml of 70 % ethanol was added to the residue and after stirring (30 min; 4 °C), the tube was centrifuged as above, and the supernatant was dried to be subsequently resuspended (in 15 ml of 70 % ethanol) and centrifuged again. Finally, the supernatant was pipetted in aliquots (1 ml each) in Eppendorf tubes and dried in Savant overnight. After weighting the pellet, each

Eppendorf was stored at −20 °C until use.

2.2. Cell cultures

Murine RAW 264.7 macrophages were acquired from the European Collection of Cell Cultures (Salisbury, UK). They were grown in Dulbecco's Modified Eagle's Medium (DMEM, Sigma-Aldrich, Milan, Italy) completed with 1 mM pyruvate, 100 mM non-essential amino acids, 10 % (v/v) heat-inactivated foetal bovine serum (FBS), penicillin (100 U/ml), streptomycin (100 μg/ml), and 1 % (w/v) L glutamine. The cells were incubated under standard conditions (37 °C, 5 % CO_2, 95 % humidity). The growth medium was changed every 2–3 days till approximately 80 % confluence was reached. All experiments were performed after a 24 h period of cell adhesion.

Human umbilical vein endothelial cells (HUVEC) were purchased from Clonetics (Lonza, Switzerland). HUVEC were cultured in an endothelial growth medium (EGM-2, Lonza, Switzerland) constituted by endothelial basal medium (EBM-2, Lonza, Switzerland) and SingleQuot Bullet Kit (Lonza, Switzerland). The cells were seeded at a density of 5000/cm^2 in T75 flasks (Corning Costar, Sigma Aldrich, St. Louis MO, USA).

U937 human myeloid leukaemia cells, purchased from LGC Standards S.r.l. (Italy), were cultured in suspension in RPMI-1640 medium (Sigma-Aldrich). Culture media were supplemented with 10 % foetal bovine serum (Euroclone, Celbio Biotecnologie, Milan, Italy), penicillin (100 units/ml), and streptomycin (100 mg/ml) (Euroclone). Cells were grown at 37 °C in T75 tissue culture flasks (Corning Inc., Corning, NY) gassed with an atmosphere of 95 % air-5 % CO_2.

2.3. Characterization of young and senescent HUVEC

HUVEC were grown by subsequent replicative passages until replicative senescence. We measured the cumulative population doubling (cPD) calculated as the sum of PD changes, according to the formula: log10(F) − log10(I))/log10(2) (Prattichizzo et al., 2018), where F is the number of cells at the end of the passage, and I is the number of seeded cells. HUVEC were classified as young (y) or senescent (s) based on replicative passages, senescence-associated (SA) ß-Galactosidase activity, and $p16^{ink4a}$ expression level. We considered yHUVEC at replicative passage <6, SA-ß-Galactosidase activity <20 %, and $p16^{ink4a}$ expression significantly lower compared to sHUVEC; whereas sHUVEC were considered at a replicative passage >15, SA-ß-Galactosidase activity >60 %, and $p16^{ink4a}$ expression significantly higher than in yHUVEC (https://doi.org/10.3390/antiox11061037).

2.4. Cell viability

MTT (3-(4,5-dimethylthiazol-2-yl)-2,5-diphenyltetrazolium bromide) assay was performed to assess cell viability of both RAW 264.7 and HUVEC. Cells ($5x10^3$/well) were grown for 24 h (RAW 264.7; yHUVEC) or 72 h (sHUVEC) at 37 °C and treated with different doses of MRME [(150–75–37.5–18.75–9.38–4.69–2.34 μg/ml; RAW 264.7), (100–50–25–12.5–6.125–3.06–1.57–0.76 μg/ml; HUVEC)]. Vehicle (70 % EtOH)-treated cells were used as control (CTRL). Briefly, 10 μl MTT (5 mg/ml) solution was added to each well (100 μl) and incubated at 37 °C for 4 h; the obtained formazan salt was solubilized by dimethyl sulfoxide (DMSO) and measured by a microplate reader at the optical density of 570 nm. Cell viability percentage was calculated according to the equation (T/C) × 100, where T and C represent the mean optical density of the treated group and the control group, respectively.

Cell viability in U937 cells was estimated with the trypan blue exclusion assay. Briefly, after treatments (i.e., 2 h incubation in culture medium in the absence or presence of 10 μg/ml MRME, then exposure for 24 h to 30 mM glucose and 0.5 ng/μl LPS alone or in combination), an aliquot of the cell suspension was diluted 1:2 (v/v) with 0.4 % trypan blue and the viable cells (i.e., those excluding trypan blue) were counted with a hemocytometer.

2.5. High glucose condition in endothelial cells and MRME treatments

Before testing MRME biological effect in high glucose (HG) condition, the anti-inflammatory activity of the extract was tested in senescent cells in normal glucose (NG) condition (D-glucose 5 mM) pretreated with the extract for 2 h, and then treated with the extract (1 μg/ml and 10 μg/ml) for 72 h. Subsequently, to investigate MRME potential in high glucose-induced inflammation, a high glucose condition (HG) was achieved by treating HUVEC as in (https://doi.org/10.3390/antiox11061037). Briefly, yHUVEC were exposed to a 45 mM D-glucose (cod. 8392, Merck, Darmstadt, Germany) medium for 24 h while sHUVEC were exposed to a 45 mM D-glucose medium for 72 h. Vehicle-treated HUVEC were grown in EGM-2 medium (D-glucose 5 mM) as control (NG). Treatments with the apple callus extract were performed for 2 h as a pretreatment, followed by 24 h treatment for yHUVEC and 72 h treatment for sHUVEC, both in HG conditions.

2.6. RNA isolation, mRNA and mature miRNAs expression by qRT-PCR

Total RNA was isolated in HUVECs and U937 using the NorgenBiotek Kit (#37500, Thorold, ON, Canada), according to the manufacturer's instructions. RNA was stored at −80 °C until use. Total RNA was reverse transcribed using PrimeScript™ RT reagent Kit with gDNA Eraser (Takara), based on the manufacturer's instructions. Quantitative real-time PCR (qRT-PCR) was performed in a Rotor-Gene Q (Qiagen) using TB Green™ Premix Ex Taq™ (Takara) in a 10 μl reaction volume. Specific primer sequences were used for qRT-PCR of the pro-inflammatory markers: IL-1β (F:CCAGCTACGAATCTCCGACC; R:CATGGCCACAACAACTGACG); MCP-1 (F:GGCTGAGACTAACCCAGAAAG; R:GGGTAGAACTGTGGTTAAGA); IL-8 (F:GGACAAGAGCCAGGAAGAAA; R:CCTACAACAGACCCACACAATA). mRNA quantification was assessed using the $2^{-\Delta Ct}$ method; β-actin was used to normalise the data. MiR-17-5p (cod: 000393, TermoFisher Scientific), miR-21-5p (cod:000397, TermoFisher Scientific), miR-126-3p (cod:000450, TermoFisher Scientific) and miR-217-5p (cod:002337, TermoFisher Scientific) expression was quantified by quantitative real-time PCR (qRT-PCR) using TaqMan miRNA assay (TermoFisher Scientific), according to the manufacturer's protocol. Data were analysed with Rotor Gene Q (Qiagen, Hilden, Germany) with the automatic comparative threshold (Ct) setting for adapting baseline. qRT-PCR data were standardised to RNU48 (cod:001006, TermoFisher Scientific). The $2^{-\Delta Ct}$ method was used to determine miRNA expression.

2.7. Nitric oxide detection

Determination of extracellular nitric oxide (NO) concentration was carried out by a UV–visible spectrophotometer. The nitrite concentration was determined according to a linear standard curve (calcium nitrite 6.25–100 μM). RAW 264.7 cells in the logarithmic phase (3×10^4 cells/100 μl) were seeded in 96-well plates and cultured for 24 h. Then, cells were co-treated for 24 h with LPS (1 μg/ml) in the absence or presence of MRME (17.88 μg/ml). Dexamethasone (DEXA) 10 μM was used as positive control. After 24 h, aliquots of 50 μl of cell culture medium were taken and incubated for 10 min in the dark at room temperature with 50 μl of Griess reagent (40 mg/ml) (Bryan & Grisham, 2007). Absorbance was measured at 570 nm using a plate reader (Bio-Rad Laboratories, Hercules, USA).

2.8. High-resolution respirometry in U937 cells

Experimental conditions to mimic either high glucose- or LPS-induced inflammation were carried out as in (Haidet et al., 2012). Briefly, 2×10^6 U937 cells were seeded in RPMI-1640 supplemented with 30 mM glucose (HG) and stimulated with 0.5 ng/μl of LPS from

E. coli for 24 h at 37 °C, 5 % of CO_2. Treatment with MRME (10 μg/ml) was performed in the culture medium for 2 h before HG, LPS, or HG + LPS stimulation. Oxygen consumption in U937 cells was monitored using an Oxygraph 2 k (O2k) high-resolution respirometer (Oroboros Instruments Corp., Austria). Prior to oxygraph measurements, cells were collected and resuspended in RPMI-1640 at 10^6 cells/ml; 2 ml of intact cells were loaded into each chamber, set to 37 °C on the magnetic stirrer. Air calibration of a polarographic oxygen sensor was performed routinely before each experiment. According to the O2k manufacturer's protocol, for all experimental conditions, basal respiration was measured in the presence of endogenous substrates. Subsequently, 5 nM (final concentration) of ATP synthase inhibitor oligomycin (Omy, Sigma) was added to measure uncoupled (non-phosphorylating) oxygen consumption. Then, the stepwise addition of 1.75 μM (final concentration) of mitochondrial oxidative phosphorylation uncoupler carbonyl cyanide 4-(trifluoromethoxy) phenylhydrazone (FCCP, Sigma), was performed to reach the maximal oxygen consumption. Finally, 2.5 μM (final concentration) of complex III inhibitor antimycin A (AmA, Sigma) was added to obtain non-mitochondrial oxygen consumption. Data analysis was performed with DatLab 7.4 software (Oroboros Instruments Corp., Austria) and the oxygen consumption rate (OCR) of intact cells was expressed as oxygen flux (pmol/s*ml).

2.9. Enzyme inhibition

2.9.1. α-glucosidase inhibition

The α-glucosidase (EC 3.2.1.20) inhibition by MRME was carried out (Lordan et al., 2013) with slight modifications. The activity of the enzyme was assessed at 405 nm by measuring the liberation of pNP (p-nitrophenol) from the substrate pNDG (p-nitrophenyl-α-D-glucopyranoside). Acarbose, a pharmacological inhibitor, was used as a reference compound, while 70 % ethanol solution as control. In a 96-well microplate, a volume of 50 μl of increasing concentrations of MRME (0.31–2.5 mg dw) or 2 mM Acarbose, and 100 μl of α-glucosidase (0.075 U/ml) in 100 mM Na-phosphate buffer at pH 6.9 was mixed and incubated for 10 min at 37 °C. Subsequently, 50 μl pNDG 5 mM was added to each well. Due to the light yellowish colour of the apple extract, a set of blanks (without the enzyme) was prepared, and the resulting absorbance was subtracted from the sample absorbance. The absorbance was measured at 405 nm using a Microplate Reader (Bio-Rad, CA, USA). Each experiment was conducted in quadruplicate, and the α-glucosidase activity was calculated using the formula:

$$\alpha\text{-glucosidase activity (\%)} = [(A_{405\ nm}\ \text{sample} - A_{405\ nm}\ \text{blank})/(A_{405\ nm}\ \text{control} - A_{405\ nm}\ \text{blank})] \times 100$$

2.9.2. α-amylase inhibition

The α-amylase inhibition by MRME was performed (Lordan et al., 2013). Equal volumes (100 μl) of 1 % (w/v) starch solution and MRME at different concentrations (0.31–2.5 mg dw) or 2 mM Acarbose were added to each tube and incubated for 10 min at 25 °C. Then, 100 μl of α-amylase (EC 3.2.1.1) from porcine pancreas 0.5 mg/ml (in 100 mM Na-phosphate buffer pH 6.9) was added to the mixture and incubated for a further 10 min at 25 °C. The α-amylase reaction was blocked by the addition of 200 μl of dinitrosalicylate reagent (1 % w/v 3,5-dinitrosalicylic acid, 0.05 % w/v sodium sulphite, 1 % w/v sodium hydroxide, and 0.25 % v/v phenol) and the mixture was boiled for 5 min and cooled at room temperature. Subsequently, from each tube, 100 μl was removed and transferred to a 96-well plate, where 100 μl of double-distilled water was added to each well. Due to the light yellowish colour of the extract, a set of blanks (without the enzyme) was prepared, and the resulting absorbance was subtracted from the sample absorbance. The absorbance was measured at 540 nm using a Microplate Reader (Bio-Rad, CA, USA). Each experiment was performed in quadruplicate and the α-amylase activity was calculated using the formula:

$$\alpha\text{-amylase activity (\%)} = [(A_{540\ nm}\ \text{sample} - A_{540\ nm}\ \text{blank})/(A_{540\ nm}\ \text{control} - A_{540\ nm}\ \text{blank})] \times 100$$

2.9.3. Lipase inhibition

The porcine pancreas lipase (EC 3.1.1.3) inhibition by MRME was performed according to (Jaradat et al., 2017) with slight modifications. 100 μl of lipase at a concentration of 1 mg/ml in 0.5 M TRIS HCl + 0.01 M $CaCl_2$, pH 7.5, was mixed with 50 μl of callus extracts at increasing concentrations (0.15–1.25 mg dw) or 5 μg Orlistat (used as positive control). The final volume was adjusted to 0.9 ml with TRIS HCl buffer, and the mixture was then incubated at 37 °C for 10 min. Subsequently, 100 μl of 10 mM 4-nitrophenyl butyrate was added to each reaction tube. The release of 2,4-dinitrophenol in the reaction was measured at 410 nm using a UV–visible spectrophotometer (Beckman CA, USA). The variation in absorbance during the 10-minute incubation period was recorded. Each data point was obtained in quadruplicate, and the lipase inhibition rate was calculated using the following formula:

$$\text{Lipase activity (\%)} = (A_{410nm}\ \text{sample} - A_{410\ nm}\ \text{blank})/(A_{410nm}\ \text{control} - A_{410nm}\ \text{blank})] \times 100$$

2.10. Statistical analysis

Statistical analysis was performed using the computer program Graph Pad Prism (v4.0, GraphPad Software Inc., San Diego, CA, USA). One-way analysis of variance (ANOVA) followed by Dunnett's or Tukey's Multiple Comparison Test was used to determine statistical differences between the experimental groups. The results are expressed as mean ± SD (Standard Deviation). Differences were considered statistically significant when $p < 0.05$.

3. Results

3.1. MRME exerts anti-inflammatory activity in RAW 264.7 cells

As a preliminary step, considering that PTAs are reported to protect against inflammation (Cui et al., 2020; Salvoza et al., 2022), the anti-inflammatory effect of MRME was evaluated in LPS-injured RAW 264.7 murine cells. Cell viability analysis showed that none of the used MRME concentrations was cytotoxic both in the absence (Fig. 1a) and presence of LPS (Fig. 1b). The evaluation of nitric oxide (NO) release, a key phenomenon in the pathogenesis of inflammation, showed a significant increase of NO concentration in LPS-treated RAW 264.7 cells, whereas co-treatment of cells with LPS (1 μg/ml) and MRME for 24 h showed a significant reduction in NO release when MRME 150 μg/ml, 75 μg/ml or 37.5 μg/ml were used (Fig. 1c).

3.2. MRME exerts an anti-inflammatory activity on senescent HUVEC

To test the anti-inflammatory effects of the apple callus extract in endothelial cells, we first assessed the cell viability of yHUVEC (Fig. 2a) and sHUVEC (Fig. 2b) by treating the cells with different MRME concentrations for 24 h and 72 h, respectively. No toxic effects of MRME were observed in yHUVEC at all doses tested (Fig. 2a), whereas a significant reduction of cell viability was observed in sHUVEC treated with high doses of MRME (i.e. 25, 50, 100 μg/ml; Fig. 2b). Thus, for the subsequent experiments we selected two concentrations both for y- and sHUVEC (1 μg/ml and 10 μg/ml) based on cell viability >80 % compared to that of the vehicle-treated cells (Control, CTRL).

Since senescent cells are characterised by a pro-inflammatory senescence-associated secretory phenotype (SASP), the modulation of

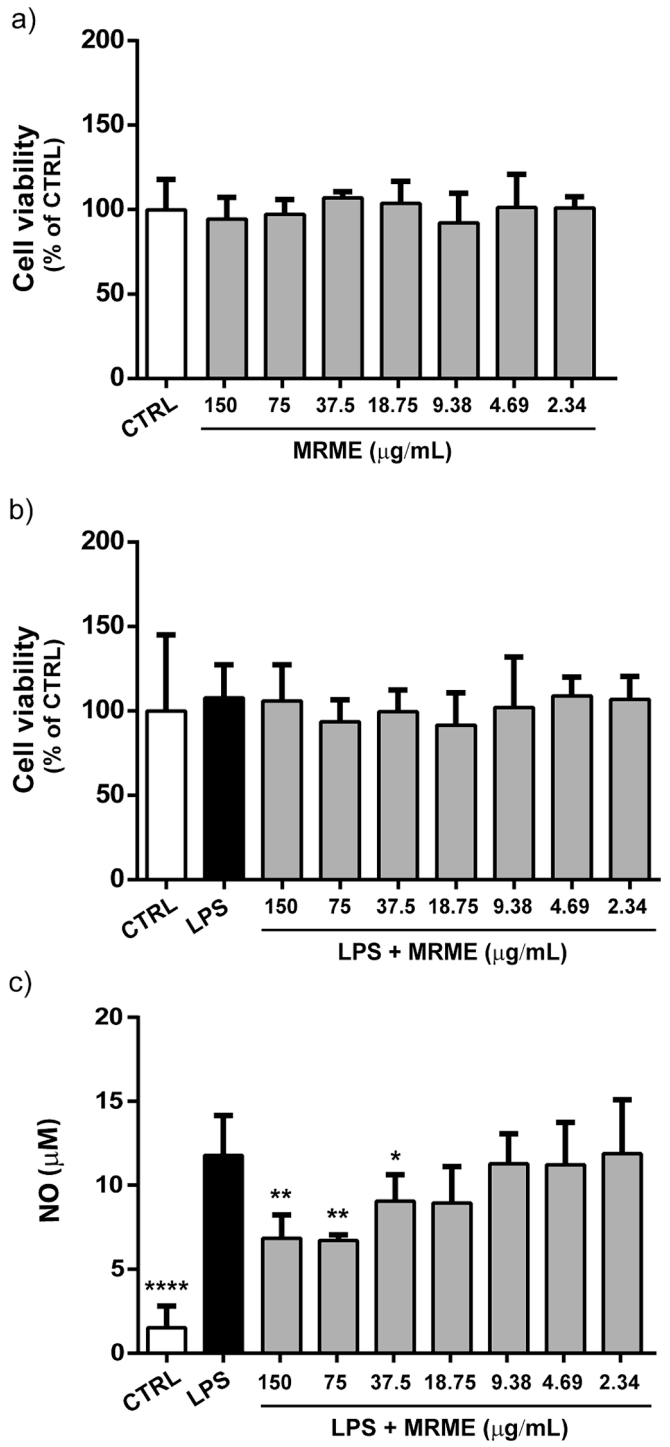

Fig. 1. MRME effects on cell viability and NO production during LPS pro-inflammatory condition. (a) RAW 264.7 cell viability after treatment with different concentrations of MRME (150–75–37.5–18.75–9.38–4.69–2.34 μg/ml) and during LPS and LPS + MRME treatments (b); (c) Nitric Oxide (NO) production (Griess Assay) in RAW 264.7 cells treated with LPS and LPS + MRME. Data are expressed as the percentage of Control (CTRL) and represent the mean ± SD of at least three independent measurements. *p < 0.05; **p < 0.01; ***p < 0.001; ****p < 0.0001 vs LPS; One-way ANOVA followed by Dunnett's multiple comparison test.

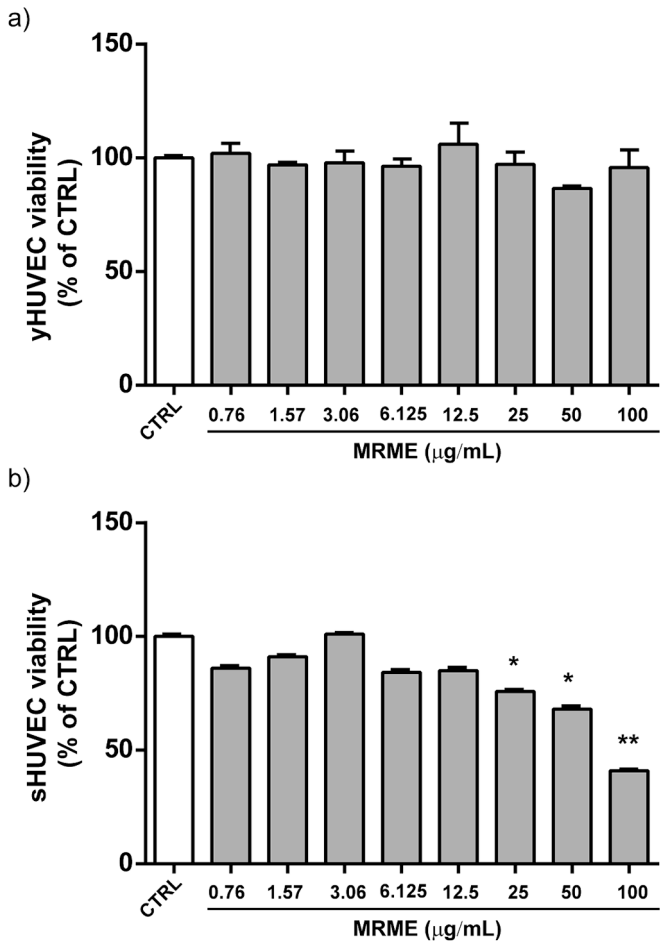

Fig. 2. Viability of yHUVEC and sHUVEC after MRME treatment. Cell viability (MTT assay) analysed in yHUVEC (a) and sHUVEC (b) treated with different concentrations of MRME (0.76–1.57–3.06–6.125–12.5–25–50–100 μg/ml), 24 h and 72 h after treatment, respectively. Results are expressed as a percentage of cell viability normalised to the viability of vehicle-treated (70 % EtOH) cells (CTRL) and presented as mean value ± SD from three independent experiments. *p < 0.05; **p < 0.01 vs CTRL; One-way ANOVA.

interleukin-8 (IL-8), interleukin-1ß (IL-1ß) and MCP-1 was evaluated only in sHUVEC. Conversely, yHUVEC, being non-inflamed, were used as a control for comparison with sHUVEC. As shown in Fig. 3, we observed a significant reduction of IL-1ß and IL-8 in sHUVEC treated with 1 μg/ml MRME for 72 h compared to vehicle-treated controls (Fig. 3a, b), while this beneficial effect was not observed when using the extract at 10 μg/ml. Although a clear trend can be seen, no significant decrease in the MCP-1 expression was found during MRME treatments (Fig. 3c).

Once the expression of the pro-inflammatory markers was evaluated after MRME treatments, the modulation of some microRNAs (namely, miR-21, miR-126, miR-17, and miR-217) was determined. More specifically, miR-21 and miR-126, belonging to the group of inflammamiRs, are able to modulate inflammatory pathways and are involved in the modulation of transcriptional programs related to the performance of endothelial cells (Matacchione et al., 2022). The oncogenic miR-17 acts pleiotropically to inhibit cellular senescence and extend longevity (Du et al., 2014), while miR-217 spreads pro-senescence signals (Mensà et al., 2020). As indicated in Fig. 4, miR-17 and miR-126 appeared significantly deregulated in sHUVEC compared to yHUVEC, while miR-217 and miR-21 expression levels were significantly augmented, in line with available literature (Dellago et al., 2013; Mensà et al., 2020; Wang et al., 2021). MRME positively affects miR-17 and miR-126 (Fig. 4a, b).

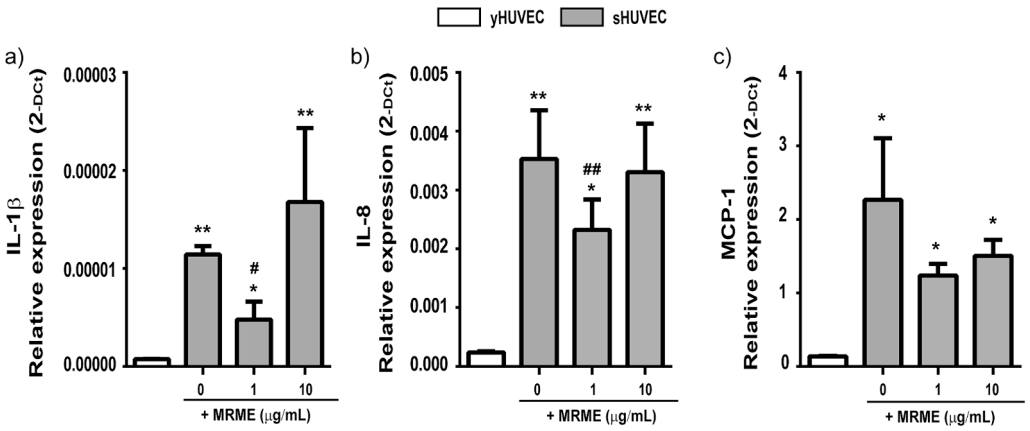

Fig. 3. MRME effect on pro-inflammatory markers in sHUVEC. Relative expression of IL-1ß (a), IL-8 (b) and MCP-1 (c) in sHUVEC after MRME treatment (1 μg/ml and 10 μg/ml). yHUVEC represent the control condition. Data are reported as relative expression levels and represent the mean ± SD of at least three independent measurements. In all panels, (*) indicates significance vs yHUVEC; (#) indicates significance versus sHUVEC; one symbol, $p < 0.05$; two symbols, $p < 0.01$; three symbols $p < 0.001$; One-way ANOVA followed by Tukey's multiple comparisons test.

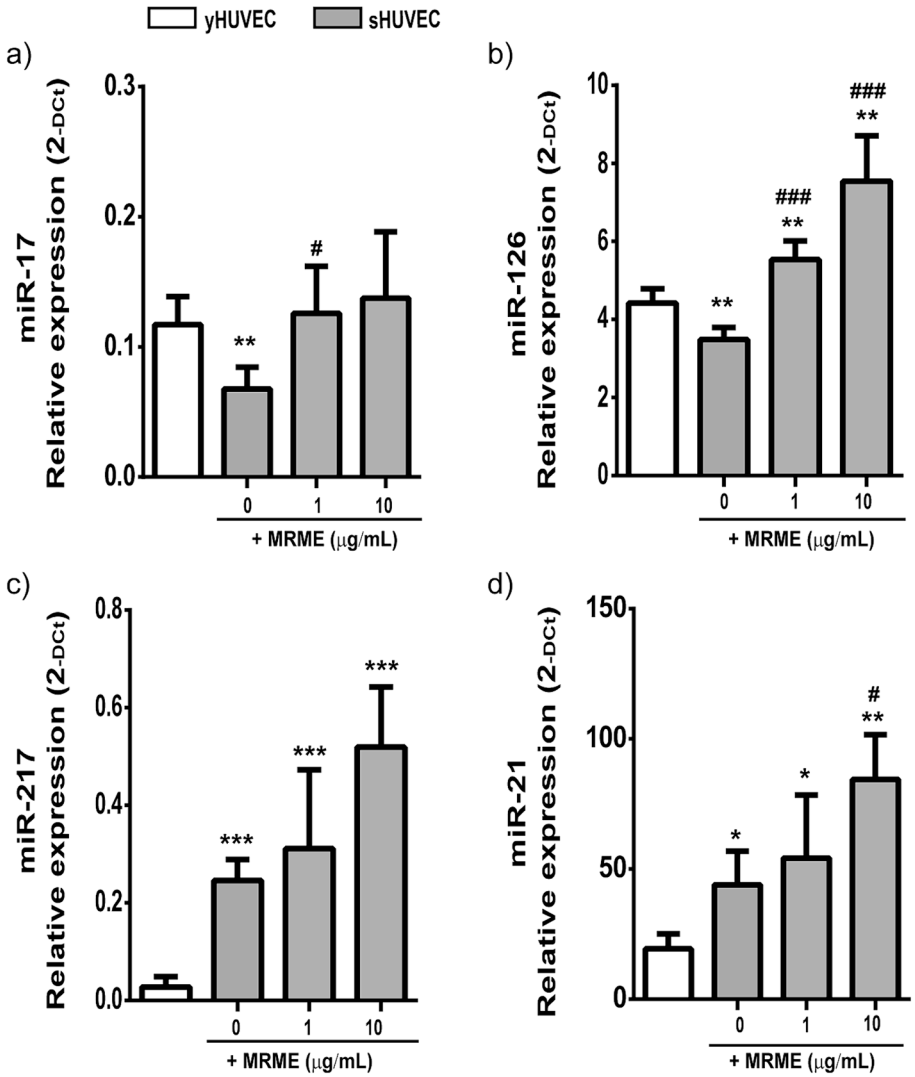

Fig. 4. MRME effects on inflammamiRNAs expression in sHUVEC. Expression of miR-17 (a), miR-126 (b), miR-217 (c), and miR-21 (d) in sHUVEC after MRME treatment (1 μg/ml and 10 μg/ml). yHUVEC are the control condition. Data are reported as relative expression levels and represent the mean ± SD of at least three independent measurements. In all panels, (*) indicates significance vs yHUVEC; (#) indicates significance vs sHUVEC; one symbol, $p < 0.05$; two symbols, $p < 0.01$; three symbols $p < 0.001$; One-way ANOVA followed by Tukey's multiple comparisons test.

Only 1 μg/ml MRME was able to significantly upregulate the miR-17 expression level in sHUVEC compared to yHUVEC (Fig. 4a), while miR-126 was found to increase with both 1 μg/ml and 10 μg/ml MRME (Fig. 4b). The other two microRNAs are not significantly modulated, with the exception of miR-21 which is upregulated after 10 μg/ml MRME treatment (Fig. 4d).

3.3. Anti-inflammatory effect of MRME on HUVEC under high glucose condition

HG exposure substantially mimics T2D, which is one of the most common age-related diseases. Following a previous study (Matacchione et al., 2022) reporting on HG-induced inflammation in y- and sHUVEC, the same model was employed to assess the extract's potential in pathological conditions characterized by glucose-induced chronic inflammation and cellular senescence. To test the anti-inflammatory effects of MRME in yHUVEC, pro-inflammatory markers expression levels were assessed in cells pretreated for 2 h with MRME (1 μg/ml and 10 μg/ml), followed by 24 h treatment with 45 mM glucose in combination with MRME (1 μg/ml and 10 μg/ml). As shown in Fig. 5, HG significantly induced IL-8, IL-1ß, and MCP-1 activity compared to NG. Both yHUVEC and sHUVEC have been used. When MRME was added to high glucose medium (45 mM), we did not observe a significantly decreased expression of IL-8 and MCP-1 as compared to HG yHUVEC alone (Fig. 5a, c), whereas 1 μg/ml MRME significantly reduced IL-1ß expression (Fig. 5b). Subsequently, MRME anti-inflammatory activity was tested in senescent cells. sHUVEC were pretreated for 2 h with MRME (1 μg/ml and 10 μg/ml), and then high glucose medium (45 mM) and MRME (1 μg/ml and 10 μg/ml) were added for 72 h. We observed that 1 μg/ml MRME was able to significantly reduce IL-8 expression level compared to HG sHUVEC (Fig. 5d), whereas we noted a significant down-regulation of IL-1ß expression only with 10 μg/ml MRME, compared to HG sHUVEC (Fig. 5e). When considering MCP-1 modulation, 10 μg/ml MRME exerts a pro-inflammatory effect ($p < 0.01$) (Fig. 5f).

3.4. MRME has a positive effect in modulating miR-217 and miR-21 expression in sHUVEC under high glucose conditions

After investigating MRME modulation of the pro-inflammatory markers, we determined the effect of the extract on miR-217, miR-17, miR-21, and miR-126 expression levels in sHUVEC under HG conditions. High glucose treatment significantly increased the expression of miR-217 and miR-21 compared to normal glucose (NG) sHUVEC but did not significantly affect the expression of miR-17 and miR-126 (Fig. 6). When HG senescent cells were treated with MRME, we observed the reduction of miR-217 and miR-21 amounts. Specifically, 1 μg/ml MRME treatment in HG sHUVEC significantly deregulated the miR-217 expression compared to HG sHUVEC, and both MRME concentration treatments reduced miR-21 expression (Fig. 6c and 6d). Interestingly, 10 μg/ml MRME significantly upregulated miR-17 expression level as compared to HG sHUVEC (Fig. 6a).

3.5. MRME protects U937 cells from LPS/high glucose stimulation

Cells of the monocyte/macrophage lineage play a pivotal role in inflammatory responses and, in addition to HUVEC, may serve as a target for studying the effects of PTAs in high glucose conditions. Building upon a previous report (Haidet et al., 2012), the potential anti-inflammatory effect of MRME under high glucose conditions was

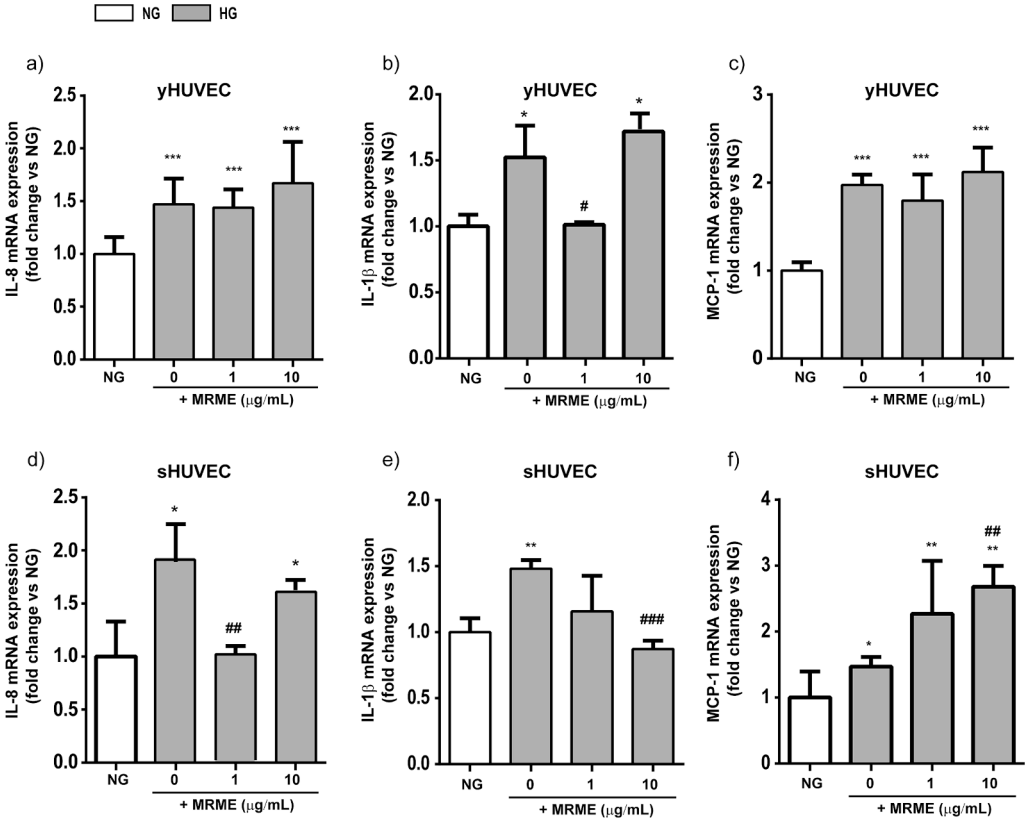

Fig. 5. MRME effects on pro-inflammatory markers in yHUVEC and sHUVEC under high glucose condition (45 mM). Relative mRNA expression of IL-8 (a, d), IL-1ß (b, e) and MCP-1 (c, f) in yHUVEC (a–c) and sHUVEC (d–f) under normal glucose (NG) condition or high glucose (HG) condition and when treated with 45 mM glucose plus MRME (1 μg/ml and 10 μg/ml). Data are reported as fold change vs untreated yHUVEC or sHUVEC and represent the mean ± SD of at least three independent measurements. In all panels, (*) indicates significance vs NG; (#) indicates significance vs HG; one symbol, $p < 0.05$; two symbols, $p < 0.01$; three symbols, $p < 0.001$; One-way ANOVA followed by Tukey's multiple comparisons test.

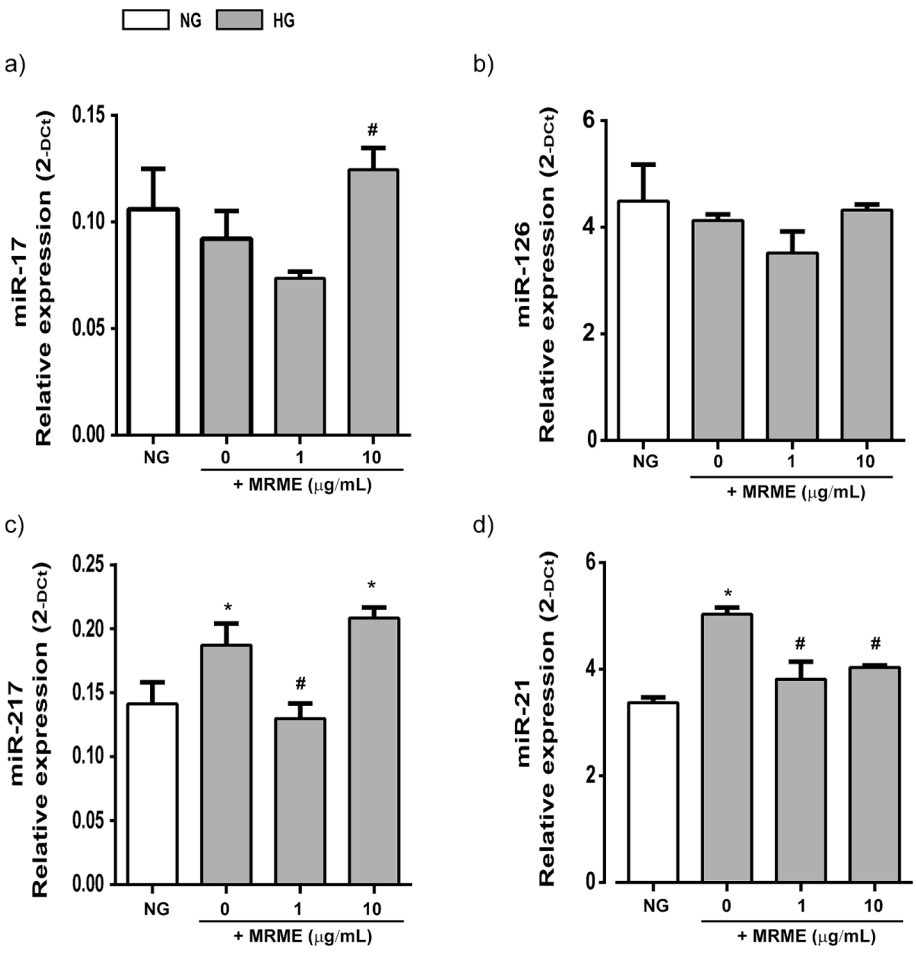

Fig. 6. MRME effect on inflammamiRNAs expression in sHUVEC under high glucose condition. Expression of miR-17 (a), miR-126 (b), miR-217 (c), and miR-21 (d) in sHUVEC under normal glucose (NG) condition or high glucose (HG) condition and HG + MRME treatment (1 μg/ml and 10 μg/ml). Data are reported as relative expression levels and represent the mean ± SD of at least three independent measurements. In all panels, (*) indicates significance vs NG; (#) indicates significance vs HG; one symbol, $p < 0.05$. One-way ANOVA followed by Tukey's multiple comparisons test.

investigated using LPS-stimulated U937 cells as a monocyte cellular model system. We found that treatment with HG and/or LPS exposure trigger in U937 cells one of the major energy pathways, the oxidative phosphorylation (oxygen consumption rate, OCR). As indicated in Fig. 7, these conditions stimulate basal respiration (Fig. 7b) accompanied by a significant enhancement of uncoupled respiration [ATP-linked respiration (Omy), Fig. 7c] and maximal respiratory capacity (FCCP) (Fig. 7d), in the absence of toxicity (Fig. 7a). It is important to underline that the responses observed with the combined exposure to HG/LPS have an additive effect of both treatments (Fig. 7b). Finally, no changes were observed on residual oxygen consumption (AmA) (Fig. 7e), suggesting that non-mitochondrial respiration was not affected by the treatments. We can postulate that HG in combination with LPS, increases oxygen demand through increased mitochondrial respiration. All these effects were prevented by MRME pre-exposure (Fig. 7 b–d). Noteworthy, MRME significantly altered the mitochondrial respiration since the basal respiration (Fig. 7b), the ATP-linked respiration (Fig. 7c), as well as the maximal respiratory capacity of the mitochondrial electron transport chain (ETC; Fig. 7d) were significantly repressed by MRME pre-treatment in the presence of HG, LPS or both (Fig. 7).

Under the same experimental conditions, inflammation markers (IL-1ß, IL-8 and MCP-1) expressions have also been analysed (Fig. 8). IL-1ß (Fig. 8a), IL-8 (Fig. 8b) and MCP-1(Fig. 8c) were positively modulated in almost all experimental conditions by MRME indicating an anti-inflammatory effect. Only IL-1ß during HG treatment didn't demonstrate an effect of MRME (Fig. 8a).

3.6. MRME inhibits α-amylase, α-glucosidase and lipase in a concentration-dependent manner

As previously mentioned (Gubitosa et al., 2024), the plant materials utilized in this study (MRM callus) exhibit a phytocomplex primarily composed of PTAs, detected in significantly higher amounts compared to those found in the pulp (as well as in the peel) of the fresh apples employed to initiate the *in vitro* culture. These SMs are known to be involved in glucose and lipid digestion (Liu et al., 2010; Yin, 2015). Thus, the effects of MRME on the enzyme activity of α-glucosidase and α-amylase (involved in carbohydrate digestion) and lipase (which plays an important role in triglycerides digestion) were evaluated. Results showed an inhibitory effect of MRME in a concentration-dependent manner. More specifically, MRME at a concentration of 2.5 mg/ml inhibits the α-glucosidase activity of about 36 % (Fig. 9a) and α-amylase activity of 76 % (Fig. 9b). The IC50 values are 2.98 ± 0.24 and 1.77 ± 0.15 mg/ml, respectively. Acarbose, a complex oligosaccharide that acts as an inhibitor, was used as a positive control. MRME at a concentration of 1.25 mg/ml inhibits lipase of 43 % (Fig. 9c) with an IC50 value of 2.06 ± 0.31 mg/ml. Orlistat was used as a standard lipase inhibitor.

4. Discussion

In the last few years, MRM callus extract (MRME) has been employed by this team in different experimental models to investigate its bioactivity. In a recent paper (Gubitosa et al., 2024) it was reported that in *in*

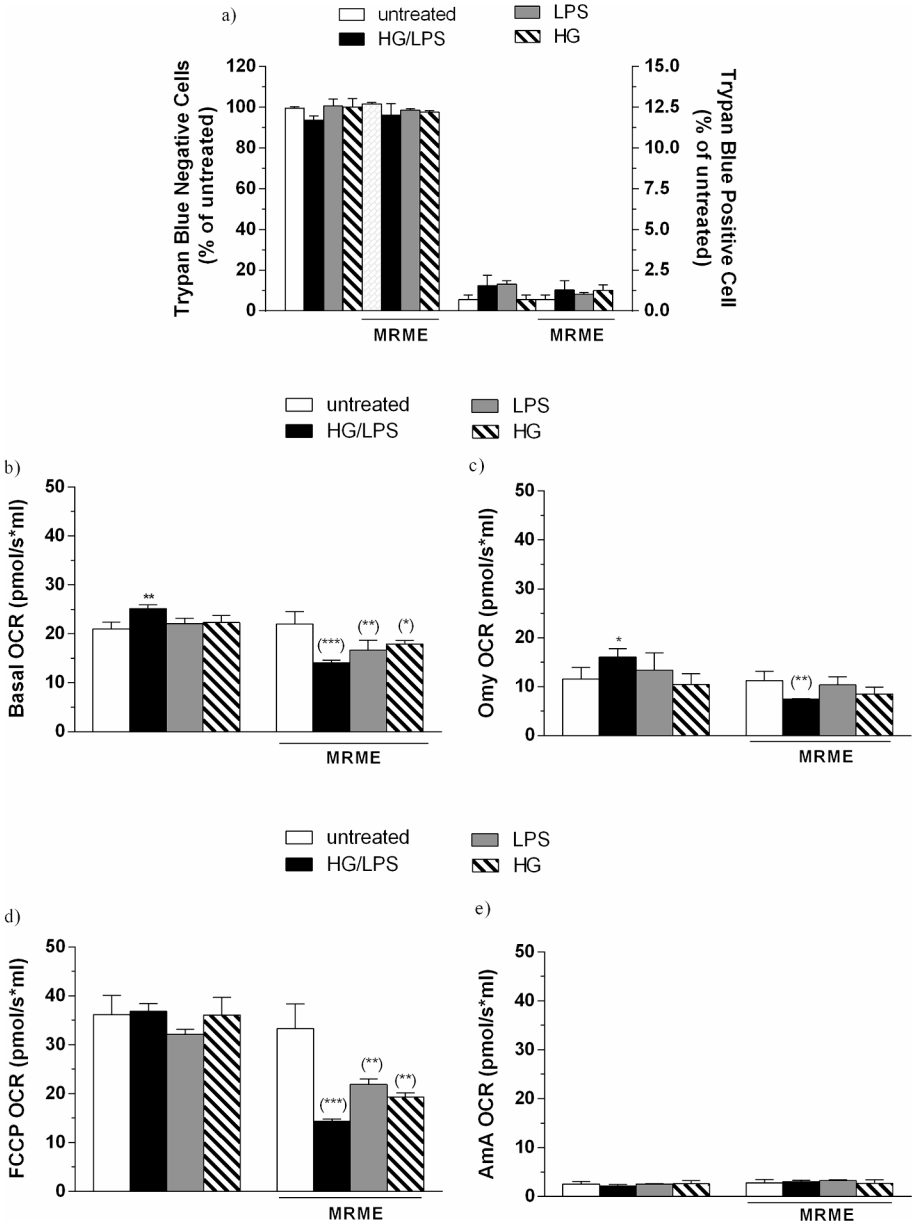

Fig. 7. MRME not only prevents the enhancing effects of high glucose condition and LPS on basal, uncoupled and maximum respiration in U937 cells, but also reduces the mitochondrial respiration without affecting cell viability. U937 cells were incubated for 2 h in the culture medium in the absence or presence of 10 μg/ml MRME, finally exposed for 24 h to 30 mM glucose (HG) and 0.5 ng/μl LPS alone or in combination. After treatments, the cells were analysed for cell viability (a) or oxygen flux (b–e) as detailed in the Materials and Methods section. Results represent the means ± SD calculated from at least three separate experiments. *$p < 0.05$, **$p < 0.01$, as compared to untreated cells (one-way ANOVA followed by Tukey's test); (*)$p < 0.05$, (**)$p < 0.01$, (***)$p < 0.003$, as compared to treated cells in the absence of MRME (one-way ANOVA followed by Tukey's test). Basal = basal respiration; Omy = ATP-linked respiration; FCCP = maximal respiratory capacity; AmA = non-mitochondrial oxygen consumption.

vitro, *ex vivo* and *in vivo* models, MRME significantly protected cells, tissues, or whole organisms from oxidative stress-induced damage. MRME is remarkably rich in PTAs (compared to the fresh apple pulp and peel, see (Gubitosa et al., 2024), and PTAs exhibit several therapeutic characteristics, including anti-inflammatory, hypoglycaemic and anti-hyperlipidemic activities (Castellano et al., 2013; Nazaruk & Borzym-Kluczyk, 2015; Oboh et al., 2021). To cite only a few interesting (certainly non-exhaustive) examples, *Potentilla chinensis*, a plant rich in tormentic acid, has been demonstrated to be strongly effective against neuro-inflammation in AD mice (Cui et al., 2020); tormentic acid was reported to ameliorate insulin resistance and to be effective for the treatment of diabetes and hyperlipidemia in high fat-fed mice (Lin et al., 2018; Wu et al., 2014); corosolic acid was shown to reduce glucose level in several *in vitro* and *in vivo* models (Xu et al., 2019) and to improve glucose metabolism in diabetic and prediabetic patients (Hibi et al., 2022). Building on this evidence, the present study was carried out to mimic *in vitro* pathological conditions characterized by glucose-induced chronic inflammation and cellular senescence (which occur in diabetic patients) and to investigate the MRME anti-inflammatory effect.

As type 2 diabetes (T2D) is an age-related disease and ageing is characterised by an increased burden of senescent cells, we aimed to address the anti-inflammatory effects of MRME not only on senescent (s-)HUVEC under high glucose (HG) but also in sHUVEC in normal glucose (NG) conditions. Pro-inflammatory markers expression levels confirmed that sHUVEC were characterised by an elevated inflammatory status, named senescence-associated secretory phenotype (SASP). When added

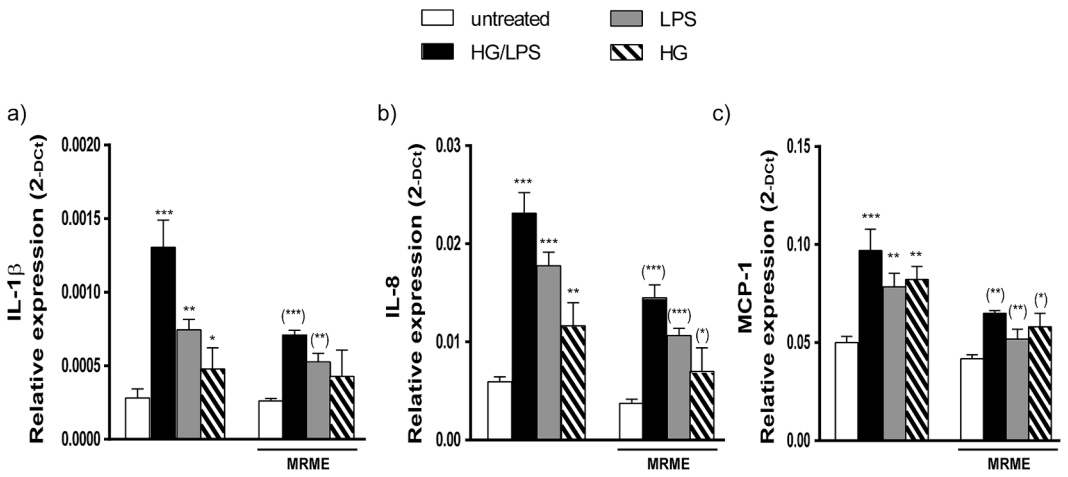

Fig. 8. Anti-inflammatory effect of MRME under high glucose condition and LPS stimulation in U937. U937 cells were incubated for 2 h in the culture medium in the absence or presence of 10 μg/ml MRME, finally exposed for 24 h to 30 mM glucose (HG) and 0.5 ng/μl LPS alone or in combination. After treatments, the cells were analysed for IL-1ß (a), IL-8 (b) and MCP-1 (c) expressions. Results represent the means ± SD calculated from three separate experiments in duplicate. Relative expression of IL-1ß (a), IL-8 (b) and MCP-1 (c) in U937 after MRME treatment (10 μg/ml). Data are reported as relative expression levels and represent the mean ± SD of at least three independent measurements. * $p < 0.05$, ** $p < 0.01$, ***$p < 0.001$, as compared to untreated cells; (*) $p < 0.05$, (**) $p < 0.01$, (***) $p < 0.001$, as compared to treated cells in the absence of MRME. One-way ANOVA followed by Tukey's multiple comparisons test.

to the culture medium, 1 μg/ml MRME was able to significantly reduce the expression of IL-8 and IL-1ß in sHUVEC. MRME treatment caused the upregulation of both miR-17 and miR-126, whereas no effects were observed on miR-217. Moreover, the mechanisms regulating the modulation of miR-21 expression levels by MRME need to be deeply investigated. Interestingly, considering IL-8 and IL-1ß, miR-17 and miR-126 modulation in sHUVEC treated with 1 μg/ml, the present results show that the extract may be considered as a senomorphic agent which can modulate the phenotype of senescent cells through interfering with inflammaging senescence-related signal pathways, without eliminating senescent cells. In this framework, MRME can mitigate the adverse effects of senescent cells altering their secretory profiles, thereby reducing inflammation and potentially improving tissue function in T2D patients.

After observing that MRME significantly reduces the LPS-induced inflammation on RAW 264.7 murine cells, we employed cultured young (y-) and senescent (s-) HUVEC exposed to a short-term glucose stimulation (24 h or 72 h, 45 mM glucose) to mimic the activation of inflammation in endothelial cells in high glucose concentration. Both in yHUVEC and sHUVEC, HG treatment induced a dramatic upregulation of IL-8, IL-1ß and MCP-1 mRNA expression compared with cells cultured in NG, confirming the HG-induced inflammatory status. MRME significantly decreased IL-1ß levels in young cells; on the other hand, it inhibited the IL-8 and IL-1ß mRNA expression in sHUVEC compared to the HG medium alone. Particularly, statistical significance was reached with a concentration of 1 μg/ml for IL-8 and 10 μg/ml for IL-1ß. This phenomenon in which different doses have different effects highlights the complexity of using natural compounds therapeutically, emphasizing the need for careful dose optimization to maximize beneficial effects while minimizing potential adverse responses. Now, the interpretation of these results remains to be clarified. In fact, we would have expected a dose-dependent effect which, as already mentioned, was not observed. To try to understand and discuss this outcome, the results obtained here are not enough. It remains an open question to be addressed in future work. Nevertheless, the level of the pro-inflammatory cytokines was decreased, and the same result was obtained in U937 cells, suggesting a mitigated inflammatory response.

The upregulation of MCP-1 observed after treatment with 10 μg/ml MRME led us to hypothesize that, in high glucose conditions, MRME might induce chemotaxis, but, in the absence of further data, consideration of this hypothesis has been postponed.

Our results also showed that MRME was able to significantly downregulate miR-217 and miR-21 expression levels which were increased in HG sHUVEC, thus pointing to an anti-inflammatory effect of MRME, especially in stress conditions. Although no modulation of miR-17 was observed under HG conditions (possibly due to short-term treatment), MRME at a concentration of 10 μg/ml increased miR-17 levels, suggesting a potential pro-longevity senomorphic effect. Available data on miR-17 modulation are contrasting, as it has been reported to be either up (Hongmei et al., 2024; Yan et al., 2019) or down (Alicka et al., 2019) regulated in response to HG levels. In addition, when examining pregnant women with gestational diabetes compared to controls, miR-17 expression levels did not differ between the two groups (Toljic et al., 2024).

Moreover, miR-126, which is commonly downregulated in diabetic patients (Olivieri et al., 2014, 2015; Rezk et al., 2016; Zampetaki et al., 2010), and so proposed as a potential predictive circulating biomarker for T2DM (Zhang et al., 2015), showed no change under the experimental conditions, consistent with previous findings in similar studies (Matacchione et al., 2022).

Based on High-Resolution Respirometry results, it could be postulated that MRME altered the functional activity of some (or all) complexes of mitochondrial ETC, since it lowered the parameters of mitochondrial function compared to the untreated (i.e., in the absence of MRME) conditions in U937 cells. It can be hypothesised that circulating monocytes can accumulate extensive damage but, nevertheless, survive because they are able to respond with the activation of a survival signaling (e.g., increased oxygen demand due to increased mitochondrial respiration) to molecules they produce and/or find in the extracellular milieu. Under this scenario, the anti-inflammatory activity ascribed to the apple callus extract could be linked to the inhibition of oxygen demand by partial mitochondrial dysfunction. Obtained results demonstrate that MRME shows an anti-inflammatory activity, which is evident also in HG condition, and can inhibit the oxygen demand in mitochondria in stress conditions, thus (likely) preventing the increase in ROS production and the consequent mitochondrial dysfunction.

Obtained results on MRME enzyme inhibitory activity showed that the callus extract exhibited the highest inhibition potential for α-amylase compared to that of the α-glucosidase. When compared to available data on the inhibitory effects of isolated triterpenes (Ding et al., 2018; Jiang et al., 2023), these data suggest a modest, although significant, inhibitory power of MRME. Similarly, also MRME inhibition of lipase activity is mild when compared to literature data (Kim et al.,

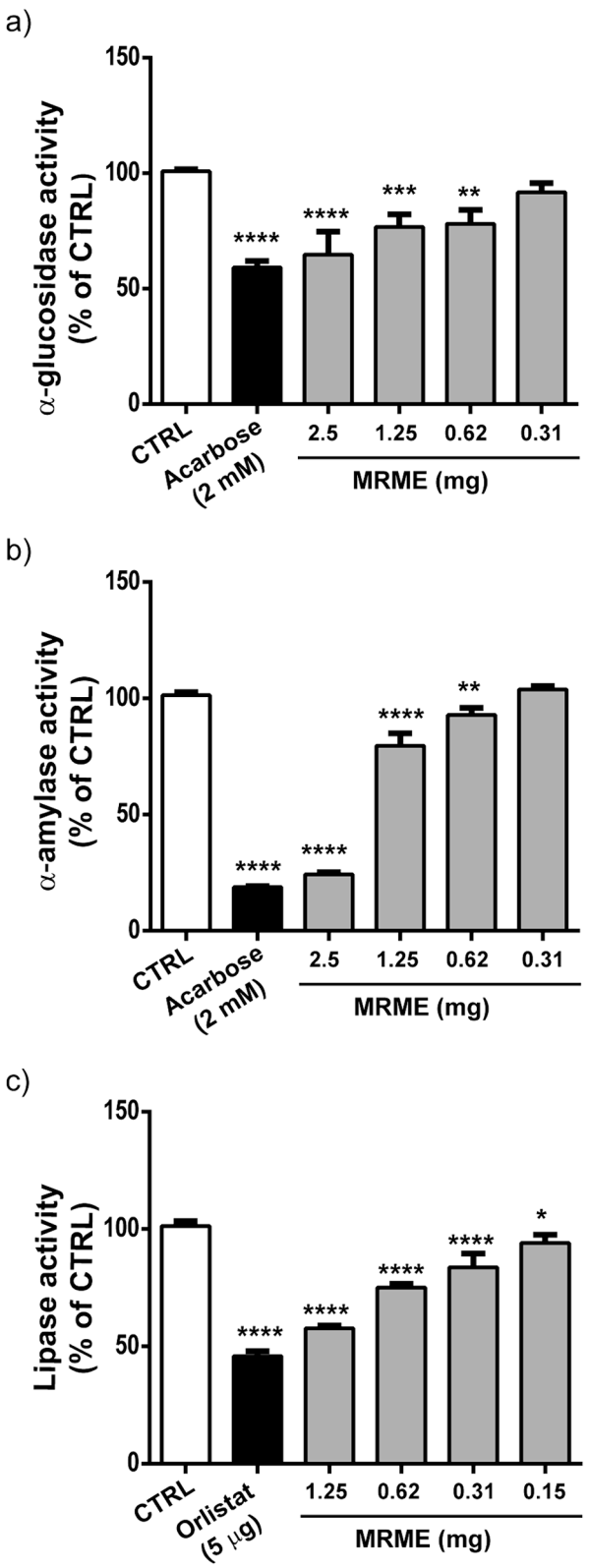

Fig. 9. Inhibitory effect of MRME on α-glucosidase, α-amylase, and lipase activities. (a) α-glucosidase activity (Acarbose 2 mM, positive control); (b) α-amylase activity (Acarbose 2 mM, positive control); (c) lipase activity (Orlistat 5 μg, positive control). Data represent the mean ± SD of four independent experiments. *$p < 0.05$;**$p < 0.01$; ***$p < 0.001$; ****$p < 0.0001$ vs Control (CTRL); One-way ANOVA followed by Multiple Comparison Test.

2009; Shen et al., 2023; Wang et al., 2020). Overall, this result (i.e., the high IC50 values of MRME) may be explained by the fact that 1 mg of dried callus extract contains only 40.81 μg of total PTAs consisting of 2.35 % oleanoic acid, 11.22 % ursolic acid, 12.86 % maslinic acid, 12.49 % corosolic acid, 1.15 % pomolic acid, 17.47 annurcoic acid and 42.44 % tormentic acid (Gubitosa et al., 2024). On the other hand, such a modest inhibition potential of MRME may be of some interest. For example, a modest inhibition of α-amylase is recommended to prevent the abnormal bacterial fermentation of undigested carbohydrates in the colon, which can lead to flatulence and diarrhoea (Etxeberria et al., 2012). On this basis, considering the mild inhibition of the three digestive enzyme activities by MRME, it is reasonable to hypothesize that the callus extract could be employed to partially inhibit the digestion process (contributing to a limited absorption and a consequently reduced calorie intake) without the most common adverse effects (gastrointestinal upset/bloating, diarrhoea, flatulence, abdominal pain) typical of the commercially available synthetic drugs (i.e., acarbose, orlistat). However, we are aware that a few issues regarding, for example, the mechanism/s of the inhibition process or the recommended daily dose of MRME still remain open questions.

Taken together, our data may be summarized as follows: (i) MRME can be used as an affordable, economic starting material to obtain high yields of pentacyclic triterpenic acids (Gubitosa et al., 2024). (ii) In line with the anti-inflammatory activity of pentacyclic triterpenic acids (see introduction), MRME showed an *in vitro* significant anti-inflammatory activity which is (likely) due to its triterpenic acids content. Based on obtained results, MRME has a positive effect on inhibition of senescence-associated inflammation, and in the presence of high glucose concentration and underlying inflammation, it shows a beneficial effect on both endothelial and immune cell dysfunction, which suggests that MRME might be of some help in decreasing the risk of developing vascular lesions, which is one of diabetes complications. (iii) MRME shows an interesting enzyme inhibitory activity which could make it potentially useful for contrasting overweight and/or obesity which are involved in diabetes development. Notably, the enzymatic inhibition activity combined with a significant anti-inflammatory effect could make MRME an interesting agent also in metabolic syndrome.

Despite some encouraging results, we are aware that many questions remain unanswered, and more research is required. Trying to fill this gap, future investigations will be carried out using the model organism *C. elegans* to test *in vivo* MRME anti-inflammatory activity and hypoglycaemic effect in order to provide further evidence that MRME could be a potential agent for maintaining good health conditions but also to test whether MRME could be of some help for the treatment of the prediabetic or diabetic condition.

Ethics statement

All subjects gave their informed consent for inclusion before they participated in the study.

Funding

This research was partly supported by the University of Urbino Carlo Bo (DISB_ALBERTINI_PROG_SIC_ALIMENTARE_2021 – DISB D.R. n.446 23.10.2020) and partly supported by the European Union—Next Generation EU—PNRR MUR project ECS_00000041-VITALITY—CUP J13C22000430001.

CRediT authorship contribution statement

Leila Benayada: Visualization, Validation, Methodology, Investigation, Formal analysis. **Federica Gubitosa:** Visualization, Validation, Methodology, Investigation, Formal analysis. **Daniele Fraternale:** Visualization, Resources, Methodology, Investigation. **Silvia Carloni:** Writing – review & editing, Writing – original draft, Visualization,

Formal analysis. **Liana Cerioni:** Writing – review & editing, Visualization, Investigation, Formal analysis. **Giulia Matacchione:** Writing – review & editing, Visualization, Methodology, Investigation, Formal analysis. **Fabiola Olivieri:** Writing – review & editing, Supervision, Data curation. **Lucia Potenza:** Validation, Supervision, Investigation, Data curation. **Roberta De Bellis:** Validation, Supervision, Methodology, Data curation. **Laura Chiarantini:** Data curation. **Carla Roselli:** Investigation, Data curation. **Laura Valentini:** Data curation. **Pietro Gobbi:** Validation, Supervision, Data curation. **Walter Balduini:** Validation, Data curation. **Noemi Pappagallo:** Validation, Supervision, Data curation. **Natascia Ventura:** Supervision, Data curation. **George E.N. Kass:** Writing – review & editing, Supervision. **Mariastella Colomba:** Writing – review & editing, Writing – original draft, Validation, Supervision, Project administration, Conceptualization. **Maria Cristina Albertini:** Writing – review & editing, Writing – original draft, Supervision, Project administration, Funding acquisition, Conceptualization.

Declaration of competing interest

The authors declare that they have no known competing financial interests or personal relationships that could have appeared to influence the work reported in this paper. The views and opinions expressed in this manuscript do not represent those of EFSA.

Data availability

No data was used for the research described in the article.

References

Alicka, M., Major, P., Wysocki, M., & Marycz, K. (2019). Adipose-derived mesenchymal stem cells isolated from patients with type 2 diabetes show reduced "Stemness" through an altered secretome profile, impaired anti-oxidative protection, and mitochondrial dynamics deterioration. *Journal of Clinical Medicine, 8*(6). https://doi.org/10.3390/jcm8060765

Bryan, N. S., & Grisham, M. B. (2007). Methods to detect nitric oxide and its metabolites in biological samples. *Free Radical Biology & Medicine, 43*(5), 645–657. https://doi.org/10.1016/j.freeradbiomed.2007.04.026

Cao, Y., Zheng, M., Sewani, M. A., & Wang, J. (2024). The miR-17-92 cluster in cardiac health and disease. *Birth Defects Research, 116*(1), Article e2273. https://doi.org/10.1002/bdr2.2273

Carantoni, M., Abbasi, F., Chu, L., Chen, Y. D., Reaven, G. M., Tsao, P. S., Varasteh, B., & Cooke, J. P. (1997). Adherence of mononuclear cells to endothelium in vitro is increased in patients with NIDDM. *Diabetes Care, 20*(9), 1462–1465. https://doi.org/10.2337/diacare.20.9.1462

Castellano, J. M., Guinda, A., Delgado, T., Rada, M., & Cayuela, J. A. (2013). Biochemical basis of the antidiabetic activity of oleanolic acid and related pentacyclic triterpenes. *Diabetes, 62*(6), 1791–1799. https://doi.org/10.2337/db12-1215

Cui, W., Sun, C., Ma, Y., Wang, S., Wang, X., & Zhang, Y. (2020). Neuroprotective effect of tormentic acid against memory impairment and neuro-inflammation in an Alzheimer's disease mouse model. *Molecular Medicine Reports, 22*(2), 739–750. https://doi.org/10.3892/mmr.2020.11154

Dellago, H., Preschitz-Kammerhofer, B., Terlecki-Zaniewicz, L., Schreiner, C., Fortschegger, K., Chang, M. W., Hackl, M., Monteforte, R., Kühnel, H., Schosserer, M., Gruber, F., Tschachler, E., Scheideler, M., Grillari-Voglauer, R., Grillari, J., & Wieser, M. (2013). High levels of oncomiR-21 contribute to the senescence-induced growth arrest in normal human cells and its knock-down increases the replicative lifespan. *Aging Cell, 12*(3), 446–458. https://doi.org/10.1111/acel.12069

Deng, J., Wang, H., Mu, X., He, X., Zhao, F., & Meng, Q. (2021). Advances in research on the preparation and biological activity of maslinic acid. *Mini Reviews in Medicinal Chemistry, 21*(1), 79–89. https://doi.org/10.2174/1389557520666200722134208

Ding, H., Hu, X., Xu, X., Zhang, G., & Gong, D. (2018). Inhibitory mechanism of two allosteric inhibitors, oleanolic acid and ursolic acid on α-glucosidase. *International Journal of Biological Macromolecules, 107*, 1844–1855. https://doi.org/10.1016/j.ijbiomac.2017.10.040

Dixon, R. A. (1985). Isolation Maintenance of Callus and Cell Suspensions Cultures. In R. R. Dixon (Ed.), *Plant Cell Culture: A Practical Approach* (pp. 1–20). Washington: IRL Press.

Du, W. W., Yang, W., Fang, L., Xuan, J., Li, H., Khorshidi, A., Gupta, S., Li, X., & Yang, B. B. (2014). miR-17 extends mouse lifespan by inhibiting senescence signaling mediated by MKP7. *Cell Death & Disease, 5*(7), Article e1355. https://doi.org/10.1038/cddis.2014.305

Etxeberria, U., de la Garza, A. L., Campión, J., Martínez, J. A., & Milagro, F. I. (2012). Antidiabetic effects of natural plant extracts via inhibition of carbohydrate hydrolysis enzymes with emphasis on pancreatic alpha amylase. *Expert Opinion on Therapeutic Targets, 16*(3), 269–297. https://doi.org/10.1517/14728222.2012.664134

Gubitosa, F., Benayada, L., Fraternale, D., De Bellis, R., Carloni, S., Potenza, L., Chiarantini, L., Gorassini, A., Verardo, G., Roselli, C., Valentini, L., Gobbi, P., Balduini, W., Ventura, N., Giannaccini, F., Kass, G. E. N., Colomba, M., & Albertini, M. C. (2024). Long-lasting bioactive compounds production from Malus x domestica Borkh var. Mela Rosa Marchigiana pulp callus culture with antioxidant activity: In vitro, ex vivo and in vivo validation. *Journal of Functional Foods, 114*, Article 106073. https://doi.org/10.1016/j.jff.2024.106073

Haidet, J., Cifarelli, V., Trucco, M., & Luppi, P. (2012). C-peptide reduces pro-inflammatory cytokine secretion in LPS-stimulated U937 monocytes in condition of hyperglycemia. *Inflammation Research, 61*(1), 27–35. https://doi.org/10.1007/s00011-011-0384-8

Heidary Navid, M., Laszczyk-Lauer, M. N., Reichling, J., & Schnitzler, P. (2014). Pentacyclic triterpenes in birch bark extract inhibit early step of herpes simplex virus type 1 replication. *Phytomedicine, 21*(11), 1273–1280. https://doi.org/10.1016/j.phymed.2014.06.007

Hibi, M., Matsui, Y., Niwa, S., Oishi, S., Yanagimoto, A., Ono, T., & Yamaguchi, T. (2022). Corosolic acid improves glucose and insulin responses in middle-aged men with impaired fasting glucose: A randomized, double-blinded, placebo-controlled crossover trial. *Journal of Functional Foods, 97*, Article 105256. https://doi.org/10.1016/j.jff.2022.105256

Hongmei, H., Maojun, Y., Ting, L. I., Dandan, W., Ying, L. I., Xiaochi, T., Lu, Y., Shi, G. U., & Yong, X. U. (2024). Neferine inhibits the progression of diabetic nephropathy by modulating the miR-17-5p/nuclear factor E2-related factor 2 axis. *Journal of Traditional Chinese Medicine, 44*(1), 44–53. https://doi.org/10.19852/j.cnki.jtcm.20231204.004

Hoogerbrugge, N., Verkerk, A., Jacobs, M. L., Postema, P. T., & Jongkind, J. F. (1996). Hypertriglyceridemia enhances monocyte binding to endothelial cells in NIDDM. *Diabetes Care, 19*(10), 1122–1125. https://doi.org/10.2337/diacare.19.10.1122

Jäger, S., Trojan, H., Kopp, T., Laszczyk, M. N., & Scheffler, A. (2009). Pentacyclic triterpene distribution in various plants – Rich sources for a new group of multi-potent plant. *Extracts, 14*(6), 2016–2031. https://www.mdpi.com/1420-3049/14/6/2016.

Jaradat, N., Zaid, A. N., Hussein, F., Zaqzouq, M., Aljammal, H., & Ayesh, O. (2017). Anti-lipase potential of the organic and aqueous extracts of ten traditional edible and medicinal plants in Palestine; a comparison study with. *Orlistat, 4*(4), Article 89. https://www.mdpi.com/2305-6320/4/4/89.

Jiang, X., Qin, Y., Wang, X., Xiong, Z., & Zhao, L. (2023). Enzyme immobilized on magnetic fluorescent bifunctional nanoparticles for α-glucosidase inhibitors virtual screening from Agrimonia pilosa Ledeb extracts accompanied with molecular modeling. *Journal of Chromatography A, 1711*, Article 464433. https://doi.org/10.1016/j.chroma.2023.464433

Jiang, Y., Wei, L., Zhang, H., Chen, Y., Gao, P., Zhang, J., Zhou, X., Zhu, S., Du, Y., Fang, C., Li, J., Feng, L., He, M., Wang, S., & Yu, J. (2022). miR-17-5p promotes glucose uptake of HTR8/SVneo trophoblast cells by inhibiting TXNIP/NLRP3 inflammasome pathway. *Diabetes, Metabolic Syndrome and Obesity, 15*, 3361–3374. https://doi.org/10.2147/dmso.S385774

Kashyap, D., Sharma, A., Punia, S., Tuli, H. S., & Sharma, A. (2016). Ursolic acid and oleanolic acid: Pentacyclic terpenoids with promising anti-inflammatory activities. *Recent Patents on Inflammation & Allergy Drug Discovery, 10*. https://doi.org/10.2174/1872213X10666160711143904

Kim, J. A., Berliner, J. A., Natarajan, R. D., & Nadler, J. L. (1994). Evidence that glucose increases monocyte binding to human aortic endothelial cells. *Diabetes, 43*(9), 1103–1107. https://doi.org/10.2337/diab.43.9.1103

Kim, J., Jang, D. S., Kim, H., & Kim, J. S. (2009). Anti-lipase and lipolytic activities of ursolic acid isolated from the roots of Actinidia arguta. *Archives of Pharmacal Research, 32*(7), 983–987. https://doi.org/10.1007/s12272-009-1702-3

Lin, C.-H., Shih, Z.-Z., Kuo, Y.-H., Huang, G.-J., Tu, P.-C., & Shih, C.-C. (2018). Antidiabetic and antihyperlipidemic effects of the flower extract of Eriobotrya japonica in streptozotocin-induced diabetic mice and the potential bioactive constituents in vitro. *Journal of Functional Foods, 49*, 122–136. https://doi.org/10.1016/j.jff.2018.08.005

Liu, J., Rajendram, R., & Zhang, L. (2010). Chapter 158 - Effects of oleanolic acid and maslinic acid on glucose and lipid metabolism: implications for the beneficial effects of olive oil on health. In V. R. Preedy, & R. R. Watson (Eds.), *Olives and olive oil in health and disease prevention* (pp. 1423–1429). Academic Press. https://doi.org/10.1016/B978-0-12-374420-3.00158-3.

Lordan, S., Smyth, T. J., Soler-Vila, A., Stanton, C., & Ross, R. P. (2013). The α-amylase and α-glucosidase inhibitory effects of Irish seaweed extracts. *Food Chemistry, 141*(3), 2170–2176. https://doi.org/10.1016/j.foodchem.2013.04.123

Martín Ortega, A. M., & Segura Campos, M. R. (2019). Chapter 13 - Bioactive compounds as therapeutic alternatives. In M. R. S. Campos (Ed.), *Bioactive Compounds* (pp. 247–264). Woodhead Publishing. https://doi.org/10.1016/B978-0-12-814774-0.00013-X.

Matacchione, G., Valli, D., Silvestrini, A., Giuliani, A., Sabbatinelli, J., Giordani, C., Coppari, S., Rippo, M. R., Albertini, M. C., & Olivieri, F. (2022). Curcumin, polydatin and quercetin synergistic activity protects from high-glucose-induced inflammation and oxidative. *Stress, 11*(6), Article 1037. https://www.mdpi.com/2076-3921/11/6/1037.

Menghini, R., Casagrande, V., Cardellini, M., Martelli, E., Terrinoni, A., Amati, F., Vasa-Nicotera, M., Ippoliti, A., Novelli, G., Melino, G., Lauro, R., & Federici, M. (2009). MicroRNA 217 modulates endothelial cell senescence via silent information regulator 1. *Circulation, 120*(15), 1524–1532. https://doi.org/10.1161/CIRCULATIONAHA.109.864629

Mensà, E., Guescini, M., Giuliani, A., Bacalini, M. G., Ramini, D., Corleone, G., Ferracin, M., Fulgenzi, G., Graciotti, L., Prattichizzo, F., Sorci, L., Battistelli, M., Monsurrò, V., Bonfigli, A. R., Cardelli, M., Recchioni, R., Marcheselli, F., Latini, S., Maggio, S., … Olivieri, F. (2020). Small extracellular vesicles deliver miR-21 and miR-217 as pro-senescence effectors to endothelial cells. *Journal of Extracellular Vesicles, 9*(1), Article 1725285. https://doi.org/10.1080/20013078.2020.1725285

Miura, T., Itoh, Y., Kaneko, T., Ueda, N., Ishida, T., Fukushima, M., Matsuyama, F., & Seino, Y. (2004). Corosolic acid induces GLUT4 translocation in genetically type 2 diabetic mice. *Biological & Pharmaceutical Bulletin, 27*(7), 1103–1105. https://doi.org/10.1248/bpb.27.1103

Mone, P., Lombardi, A., Kansakar, U., Varzideh, F., Jankauskas, S. S., Pansini, A., Marzocco, S., De Gennaro, S., Famiglietti, M., Macina, G., Frullone, S., & Santulli, G. (2023). Empagliflozin improves the microRNA signature of endothelial dysfunction in patients with heart failure with preserved ejection fraction and diabetes. *The Journal of Pharmacology and Experimental Therapeutics, 384*(1), 116–122. https://doi.org/10.1124/jpet.121.001251

Nazaruk, J., & Borzym-Kluczyk, M. (2015). The role of triterpenes in the management of diabetes mellitus and its complications. *Phytochemistry Reviews, 14*(4), 675–690. https://doi.org/10.1007/s11101-014-9369-x

Nkuimi Wandjou, J. G., Mevi, S., Sagratini, G., Vittori, S., Dall'Acqua, S., Caprioli, G., Lupidi, G., Mombelli, G., Arpini, S., Allegrini, P., Les, F., López, V., & Maggi, F. (2020). Antioxidant and enzyme inhibitory properties of the polyphenolic-rich extract from an ancient apple variety of Central Italy (Mela Rosa dei Monti Sibillini). *Plants (Basel), 9*, Article 9. https://doi.org/10.3390/plants9010009

Oboh, M., Govender, L., Siwela, M., & Mkhwanazi, B. N. (2021). Anti-diabetic potential of plant-based pentacyclic triterpene derivatives: progress made to improve efficacy and bioavailability. *Molecules, 26*(23).

Olivieri, F., Bonafè, M., Spazzafumo, L., Gobbi, M., Prattichizzo, F., Recchioni, R., Marcheselli, F., La Sala, L., Galeazzi, R., Rippo, M. R., Fulgenzi, G., Angelini, S., Lazzarini, R., Bonfigli, A. R., Brugè, F., Tiano, L., Genovese, S., Ceriello, A., Boemi, M., & Testa, R. (2014). Age- and glycemia-related miR-126-3p levels in plasma and endothelial cells. *Aging (Albany NY), 6*(9), 771–787. https://doi.org/10.18632/aging.100693

Olivieri, F., Spazzafumo, L., Bonafè, M., Recchioni, R., Prattichizzo, F., Marcheselli, F., Micolucci, L., Mensà, E., Giuliani, A., Santini, G., Gobbi, M., Lazzarini, R., Boemi, M., Testa, R., Antonicelli, R., Procopio, A. D., & Bonfigli, A. R. (2015). MiR-21-5p and miR-126a-3p levels in plasma and circulating angiogenic cells: relationship with type 2 diabetes complications. *Oncotarget, 6*(34). https://www.oncotarget.com/article/6164/text/%J Oncotarget.

Patil, B. S., Jayaprakasha, G. K., Chidambara Murthy, K. N., & Vikram, A. (2009). Bioactive compounds: Historical perspectives, opportunities, and challenges. *Journal of Agricultural and Food Chemistry, 57*(18), 8142–8160. https://doi.org/10.1021/jf9000132

Pillai, N., Soumya, P., Saraswathy, M., Sivan, K. S., Mondal, S., & Np, S. (2021). Bioactive compounds in functional food and their role as therapeutics. *Bioactive Compounds in Health and Disease, 4*, 24–39. https://doi.org/10.31989/bchd.v4i3.786

Potenza, L., Minutelli, M., Stocchi, V., & Fraternale, D. (2020). Biological potential of an ethanolic extract from "Mela Rosa Marchigiana" pulp callus culture. *Journal of Functional Foods, 75*, Article 104269. https://doi.org/10.1016/j.jff.2020.104269

Prattichizzo, F., De Nigris, V., Mancuso, E., Spiga, R., Giuliani, A., Matacchione, G., Lazzarini, R., Marcheselli, F., Recchioni, R., Testa, R., La Sala, L., Rippo, M. R., Procopio, A. D., Olivieri, F., & Ceriello, A. (2018). Short-term sustained hyperglycaemia fosters an archetypal senescence-associated secretory phenotype in endothelial cells and macrophages. *Redox Biology, 15*, 170–181. https://doi.org/10.1016/j.redox.2017.12.001

Qin, B., Yang, H., & Xiao, B. (2012). Role of microRNAs in endothelial inflammation and senescence. *Molecular Biology Reports, 39*(4), 4509–4518. https://doi.org/10.1007/s11033-011-1241-0

Rezk, N. A., Sabbah, N. A., & Saad, M. S. (2016). Role of MicroRNA 126 in screening, diagnosis, and prognosis of diabetic patients in Egypt. *IUBMB Life, 68*(6), 452–458. https://doi.org/10.1002/iub.1502

Salvoza, N., Giraudi, P. J., Tiribelli, C., & Rosso, N. (2022). Natural compounds for counteracting nonalcoholic fatty liver disease (NAFLD): Advantages and limitations of the suggested candidates. *International Journal of Molecular Sciences, 23*(5), Article 2764. https://www.mdpi.com/1422-0067/23/5/2764.

Shen, H., Wang, J., Ao, J., Ye, L., Shi, Y., Liu, Y., Li, M., & Luo, A. (2023). The inhibitory mechanism of pentacyclic triterpenoid acids on pancreatic lipase and cholesterol esterase. *Food Bioscience, 51*, Article 102341. https://doi.org/10.1016/j.fbio.2022.102341

Shrinet, K., Singh, R. K., Chaurasia, A. K., Tripathi, A., & Kumar, A. (2021). Chapter 17 - Bioactive compounds and their future therapeutic applications. In R. P. Sinha, & D.-P. Häder (Eds.), *Natural bioactive compounds* (pp. 337–362). Academic Press. https://doi.org/10.1016/B978-0-12-820655-3.00017-3.

Tang, Y., Chen, Y., Guo, Q., Zhang, L., Liu, H., Wang, S., Wu, X., Shen, X., & Tao, L. (2023). MiR-126-loaded immunoliposomes against vascular endothelial inflammation in vitro and vivo evaluation. *Pharmaceutics, 15*(5). https://doi.org/10.3390/pharmaceutics15051379

Toljic, M., Nikolic, N., Joksic, I., Carkic, J., Munjas, J., Karadzov Orlic, N., & Milasin, J. (2024). Expression of miRNAs and proinflammatory cytokines in pregnant women with gestational diabetes mellitus. *Journal of Reproductive Immunology, 162*, Article 104211. https://doi.org/10.1016/j.jri.2024.104211

Verardo, G., Gorassini, A., & Fraternale, D. (2019). New triterpenic acids produced in callus culture from fruit pulp of Acca sellowiana (O. Berg) Burret. *Food Research International, 119*, 596–604. https://doi.org/10.1016/j.foodres.2018.10.037

Verardo, G., Gorassini, A., Ricci, D., & Fraternale, D. (2017). High triterpenic acids production in callus cultures from fruit pulp of two apple varieties. *Phytochemical Analysis, 28*(1), 5–15. https://doi.org/10.1002/pca.2638

Wang, L., Guan, X.-Q., He, R.-J., Huo, P.-C., Qin, W.-W., Cui, L.-T., Hu, Q., Hou, J., Mamat, M., Jia, S.-N., Tang, H., & Ge, G.-B. (2020). Discovery and characterization of pentacyclic triterpenoid acids in Styrax as potent and reversible pancreatic lipase inhibitors. *Journal of Functional Foods, 74*, Article 104159. https://doi.org/10.1016/j.jff.2020.104159

Wang, Z., Shi, D., Zhang, N., Yuan, T., & Tao, H. (2021). MiR-217 promotes endothelial cell senescence through the SIRT1/p53 signaling pathway. *Journal of Molecular Histology, 52*(2), 257–267. https://doi.org/10.1007/s10735-020-09945-x

Wu, J.-B., Kuo, Y.-H., Lin, C.-H., Ho, H.-Y., & Shih, C.-C. (2014). Tormentic acid, a major component of suspension cells of Eriobotrya japonica, suppresses high-fat diet-induced diabetes and hyperlipidemia by glucose transporter 4 and AMP-activated protein kinase phosphorylation. *Journal of Agricultural and Food Chemistry, 62*(44), 10717–10726. https://doi.org/10.1021/jf503334d

Xiao, S., Tian, Z., Wang, Y., Si, L., Zhang, L., & Zhou, D. (2018). Recent progress in the antiviral activity and mechanism study of pentacyclic triterpenoids and their derivatives. *Medicinal Research Reviews, 38*(3), 951–976. https://doi.org/10.1002/med.21484

Xu, S., Wang, G., Peng, W., Xu, Y., Zhang, Y., Ge, Y., Jing, Y., & Gong, Z. (2019). Corosolic acid isolated from Eriobotrya japonica leaves reduces glucose level in human hepatocellular carcinoma cells, zebrafish and rats. *Scientific Reports, 9*(1), 4388. https://doi.org/10.1038/s41598-019-40934-7

Yan, M., Chen, K., Sun, R., Lin, K., Qian, X., Yuan, M., Wang, Y., Ma, J., Qing, Y., Xu, J., Wei, M., Huang, D., & Li, J. (2019). Glucose impairs angiogenesis and promotes ventricular remodelling following myocardial infarction via upregulation of microRNA-17. *Experimental Cell Research, 381*(2), 191–200. https://doi.org/10.1016/j.yexcr.2019.04.039

Yin, M. C. (2015). Inhibitory effects and actions of pentacyclic triterpenes upon glycation. *Biomedicine (Taipei), 5*(3), 13. https://doi.org/10.7603/s40681-015-0013-x

Zampetaki, A., Kiechl, S., Drozdov, I., Willeit, P., Mayr, U., Prokopi, M., Mayr, A., Weger, S., Oberhollenzer, F., Bonora, E., Shah, A., Willeit, J., & Mayr, M. (2010). Plasma microRNA profiling reveals loss of endothelial miR-126 and other microRNAs in type 2 diabetes. *Circulation Research, 107*(6), 810–817. https://doi.org/10.1161/circresaha.110.226357

Zhang, T., Li, L., Shang, Q., Lv, C., Wang, C., & Su, B. (2015). Circulating miR-126 is a potential biomarker to predict the onset of type 2 diabetes mellitus in susceptible individuals. *Biochemical and Biophysical Research Communications, 463*(1–2), 60–63. https://doi.org/10.1016/j.bbrc.2015.05.017

Zhang, M., Xue, X., Lou, Z., Lin, Y., Li, Q., & Huang, C. (2024). Exosomes from senescent epithelial cells activate pulmonary fibroblasts via the miR-217-5p/Sirt1 axis in paraquat-induced pulmonary fibrosis. *Journal of Translational Medicine, 22*(1), 310. https://doi.org/10.1186/s12967-024-05094-x